Highly Sensitive SERS Detection of Neonicotinoid Pesticides. Complete Raman Spectral Assignment of Clothianidin and Imidacloprid

Niamh Creedon[1], Pierre Lovera[1], Julio Gutierrez Moreno[2], Michael Nolan[2] and Alan O'Riordan[1]*

1: Nanotechnology Group, Tyndall National Institute, University College Cork, Lee Maltings, Cork, T12 R5CP, Ireland.

2: Materials Modelling for Devices Group, Tyndall National Institute, University College Cork, Lee Maltings, Cork, T12 R5CP, Ireland.

E-mail: alan.oriordan@tyndall.ie

Abstract:

The use of Surface Enhanced Raman Spectroscopy in the development of low cost, portable sensor devices that can be used in the field for nitroguanidine neonicotinoid insecticide detection is appealing. However, a key challenge to achieving this goal is the lack of detailed analysis and vibrational assignment for the most popular neonicotinoids. To make progress towards this goal, this paper presents an analysis of the bulk Raman and SERS spectra of two neonicotinoids, namely clothianidin and imidacloprid. Combined with first principles simulations, this allowed assignment of all Raman spectral modes for both molecules. To our knowledge, this is the first report of SERS analysis and vibrational assignment of Clothianidin and a comprehensive assignment and analysis is provided for imidacloprid. Silver nanostructured surfaces were fabricated for qualitative SERS analysis, which provides the characteristic spectra of the target molecules, and demonstrates the ability of SERS to sense these molecules at concentrations as low as 1 ng/L. These detection limits are significantly lower than reported solid state electrochemical techniques and are on a par with high-end chromatographic-mass spectroscopy laboratory methods. These SERS sensors thus allow for the selective and sensitive detection of neonicotinoids, and provides complementary qualitative and quantitative data for the molecules. Furthermore, this technique can be adapted to portable devices for remote sensing applications. Further work focuses on integrating our device with an electronics platform for truly portable residue detection.

Keywords: Clothianidin; Imidacloprid; Raman Spectroscopy; SERS, Pesticides; Raman Spectral Assignment, First Principle Simulations

1. Introduction

The requirements for pest control in intensive agriculture systems has driven the growth of insecticide use within the agri-sector. In this regard, neonicotinoids are a relatively powerful class of insecticide. Imidacloprid was introduced in 1991 and the neonicitinoids have been the fastest-growing class of insecticides in modern crop protection,[1] taking *ca.* 17% of the global insecticide market.[2] Neonicotinoids target the nicotinic acetylcholine receptors in insects [3] and are extremely effective against herbivorous insects. The perceived low toxicity to mammals, birds and fish,[4] led to their widespread uptake for use on a variety of crops.

However recent years have seen significant concerns raised about the environmental impact of neonicotinoids on the global pollinator population, including honey bees, bumble bees and solitary bees. It is claimed that neonicotinoids affect the homing capacity of honey bees and their reproductive ability with the result of colony collapse disorder. [5, 6] Another emerging concern is that human exposure to these pesticides may increase the prevalence of some cancers,[7, 8] respiratory diseases [9, 10] and damage to the reproductive system, nervous system and liver [11, 12], while children are particularly at risk.[13] As a consequence, this class of insecticides has become the subject of a world-wide debate.[14, 15] The European Food Safety Authority (EFSA), recognising the potential threat caused by neonicotinoids, enforced a temporary ban by the European Union in 2013.[16] The maximum allowable residue limits of neonicotinoids was set to between 0.01 and 3 mg/kg for many fruits and vegetables.[17, 18] Ecological and human health risk assessments for selected neonicotinoids, Imidacloprid and Clothianidin were reviewed by the EFSA in 2018 and the assessment concluded that the use of neonicotinoid pesticides on outdoor crops presents a risk to wild bees and honeybees.[19] Consequently, in 2019, EU governments passed a near-total ban on the use of active neonicotinoid pesticides including clothianidin and imidacloprid on outdoor crops due to their impact on pollinators. To effectively enforce this ban the development of easy-to-use and low maintenance portable sensor devices is required to enable rapid and reliable decentralised detection of these pesticides.

Current techniques for the detection of neonicotinoids include both chemical and optical detection methods: enzyme linked immuno-sorbent assays (ELISA),[20, 21] HPLC- or GC- mass spectrometry,[17, 22-25] voltammetric methods,[26-29] and fluorescence spectroscopy.[30] While these techniques can detect insecticides at low concentrations (low parts per billion), the associated instruments are complex, have a high cost of ownership and are cannot be used for remote field analysis. To permit rapid detection of these neonicotinoids in the field (*in situ*) necessitates the development of portable, low cost sensor devices. This can be realised using a single optical technique, namely surface enhanced Raman spectroscopy (SERS), which permits the necessary quantitative detection of the target species,

and trace analyte detection. Raman spectroscopy uses the vibrational properties of the compounds of interest, providing a spectral finger print of the molecule.[31-34] SERS enhancement occurs at nanostructured plasmonic surfaces following illumination with monochromatic radiation which arises from (i) an increase in local electromagnetic field strengths of localized surface plasmons (in nanogaps between metal clusters called "hot spots") and (ii) chemical resonant energy charge transfer In addition, SERS provides high sensitivity, rapid analysis time and little background interference from water molecules.

With this in mind, the present paper focuses on the development and use of SERS for the detection of the neonicotinoids clothianidin and imidacloprid as test cases for the wider application of SERS as a suitabledetection techniques for neonicotinoids. Bulk Raman studies were performed to explore the characteristic Raman modes to give a fingerprint for both molecules. A silver nanostructured polymer substrate was fabricated for SERS characterisation, which provides physical data (vibrational spectrum) for the insecticide solutions. Molecular identification was verified using SERS together with high level density functional theory simulations. This SERS sensor can be adapted for use in a single portable device. Integration into a portable devices is beyond the scope of this paper which aims to demonstrate the ability of SERS to discriminate between the molecules of interest and determine their concentration down to ultra low limits of detection which are competitive with or better than other technologies.

2. Experimental

2.1. Materials and Reagents

Polyvinylidene fluoride (PVDF), silver wire, imidacloprid and clothianidin were purchased from Sigma-Aldrich and used as received. Deionized water (18.2 MΩ cm) from an ELGA Pure Lab Ultra system was used for the preparation of samples.

2.2. SERS Substrate Fabrication

Pellets of PVDF were placed on a microscope slide and melted on a hotplate at ~220°C. An aluminium (Al) master template was prepared as previously described by Creedon et al. [35]. The Al master was placed onto the melted droplet and pushed downward so the PVDF wetted the Al surface. The glass slide was removed from the hotplate and the PVDF was peeled from both the glass slide and Al template, to yield a nanostructured polymer base. To complete the substrate fabrication, a thin silver

layer (30 nm) was deposited onto the PVDF base by thermal evaporation (Edwards Autocore 500, 3×10^{-7} bar, ~1.6 A). The thickness and the deposition rate were controlled in situ using a calibrated quartz microbalance.

2.3. Microscopic and Raman Characterisation

Optical micrographs were acquired using a calibrated microscope (Axioskop II, Carl Zeiss Ltd.) equipped with a charge-coupled detector camera (CCD; DEI-750, Optronics). Scanning electron microscopy analysis was undertaken to characterize the SERS sensor surface after the fabrication procedure. SEM images were acquired using a calibrated field emission SEM (JSM-7500F, JEOL UK Ltd.) operating at beam voltages between 3 and 5 kV. All Raman measurements were recorded using a Confocal Renishaw Raman Microscope equipped with a 514 nm Ar ion laser and analysed using Wire 3.0 computer software. The laser spot diameter was ~1 μm at the substrate surface and a laser power density of ~7×10^{4} W/cm^{2} was used. SERS spectra collected using a 50x magnification (0.75 NA) objective microscope, with a data acquisition time of 10 s, over an extended spectral range of 200 cm^{-1} to 3500 cm^{-1}. The spectrometer was equipped with a computer controlled motorised XYZ stage employed to focus and adjust the positioning of the sample on the silver surface. Subtraction of the baseline was performed on all spectra to eliminate background noise from the underlying polymer and the recorded spectra were imported into Origin® 7.4 (OriginLab) to facilitate data analysis.

2.4. Computational Methodology

Density functional theory (DFT) calculations were undertaken to find the equilibrium molecular structures and aid the assignment of the Raman modes of the isolated imidacloprid and clothianidin molecules. The hybrid exchange-correlation functional B3-LYP, using Becke's three parameter exchange and Lee–Yang–Parr correlation [36] was used along with a triple-ζ valence basis set which has two sets of polarization functions, TVZPP [37]. These are implemented in the Turbomole 6.4 code.[38] The dispersion forces were corrected by the Grimme's DFT-D3 method.[39] Redundant internal coordinates were used for the geometry optimization with energy and gradient convergence criteria of less than 10^{-6} Hartree and 0.002 Hartree/Bohr. [40] Force constant calculations were implemented to estimate the vibrational modes of the isolated imidacloprid and clothianidin molecules and harmonic vibrational frequencies were estimated by the analytical evaluation of second derivatives of the energy.[41, 42] A scaling factor of 0.9669 was applied to the fundamental vibrational frequencies to correct for the error due to the harmonic approximation in the theoretical model. [43]

2.5. Analysis of Neonicotinoids

Working solutions of both imidacloprid and clothianidin were prepared in a methanol– DI water solution (1:1) and diluted to 10 μg/mL and 1 ng/mL concentrations. Solutions were then deposited (50 μl) via a drop/dry process onto the SERS substrates (10 min). All samples were thoroughly rinsed with DI water before Raman analysis to remove unadsorbed, clumped molecules that accumulated on the surface of the substrate during the drying process. Bulk Raman spectra were also acquired for both molecules. In this work, all wavenumbers in the discussion section are related to the Raman spectra, unless otherwise stated.

3. Results and Discussion

3.1. SERS substrate Characterisation

A typical SEM micrograph of a portion of a fully prepared PVDF substrate, following Ag deposition, is shown in Figure 1. From SEM analysis the size distribution of the Ag nano-structures is estimated at 60 ± 20 nm while the gaps between the clusters are *ca.* 10 ± 5 nm. The small separation between Ag clusters delivers a high yield of electromagnetic hot-spots, making them very attractive and suitable for SERS sensing. A model compound, crystal violet, was analysed to characterise the SERS capabilities of the substrate and the results of this characterisation are presented in Supp. Info (Figure S1), while further substrate characterisation was explored in significant detail in Ref. [35] These substrates demonstrated high sensitivity to crystal violet yielding enhancement factors of ~10^6.

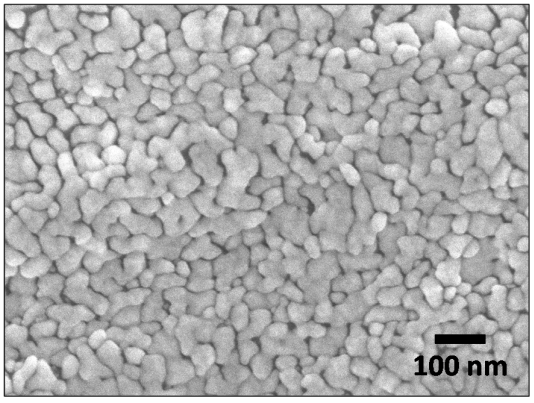

Figure 1: SEM image of a portion of the fabricated SERS substrate silver surface.

3.2. Raman and SERS Analysis of Clothianidin

Bulk Raman spectra were first acquired for Clothianidin and the Raman spectrum is shown in Figure 2 (a), exhibiting all the expected characteristic peaks of this molecule. Clothianidin consists of a chloro-thiazole ring linked by a carbon to a nitroguanidine structure. The structure of clothianidin together with the atomic numbering used in the later discussion is given in Figure 2 (c). The strongest Raman peaks were identified and assigned to their corresponding vibrational modes by visualization of the vibrational modes from the DFT calculations and comparison to the corresponding vibrations in similar molecules in the literature[44, 45] and the assignments are shown in Table 1. In general, the scaled DFT frequencies for the vibrational modes are in good agreement with the experimental vibrational frequencies. The full set of Raman assignments for Clothianidin are discussed in detail in the Supporting Information (SI, Section S2).

C-H vibrations

The C-H stretching vibrations observed in the spectral range from ~3000 - 3600 cm^{-1} are presented in Table S1 (SI, Section 2) and we discuss the most relevant modes here. The Raman band at 3121 cm^{-1} is assigned to the C-H stretch in the chlorothiazole ring, C13-H19. There are in-plane bending vibrations associated with C13-H at 1532 cm^{-1}, 1296 cm^{-1}, 1248 cm^{-1} and 1152 cm^{-1}. The out of plane wagging modes for C13-H are observed at 871 cm^{-1} and 669 cm^{-1}. The C10-H symmetric and asymmetric stretching modes are observed at 2965 cm^{-1} and 3011 cm^{-1}, respectively and the bending mode is at 1462 cm^{-1}. Multiple out of plane twisting modes were found at 1422 cm^{-1}, and 1051 cm^{-1}. Finally Raman bands at 947 cm^{-1}, 669 cm^{-1} and 259 cm^{-1} can be assigned to the in-plane rocking of H16 and H17 with C10. The methyl C-H symmetric and asymmetric stretching modes are observed at 2860 cm^{-1} and 2900 cm^{-1}, respectively, while the in-plane bending and wagging modes of methyl are found at 1422 cm^{-1} and 992 cm^{-1}.

Ring Vibrations

C-C and N-C stretching modes are found at at 1532 cm^{-1} and 1433 cm^{-1} and can be assigned to ring C13-C11 and N7-C14 bonds. A strong asymmetric stretch between C14-S2, Cl1 is assigned to the 992 cm^{-1} band. The observed band at 594 cm^{-1} is assigned to the out of plane wagging modes of the chlorothiazole ring and other out-of-plane wagging modes are at 443 cm^{-1} and 358 cm^{-1}. The stretching vibrational mode for the C14-Cl1 bond is seen at 432.6 cm^{-1} in the SERS spectra and is

agreement with the literature data.[46] Raman peaks at 259 cm^{-1} and 358 cm^{-1} are assigned to the weak bending and wagging mode of C-Cl, respectively.

N-O, N-H and C-N Vibrations

The N9-O symmetric and asymmetric stretching vibrations occur at 1318 cm^{-1} and 1570 cm^{-1}, respectively, which are typical for nitroalkane stretching as reported in the literature.[46, 47] The wagging out of plane vibration of N9-O appears at 754 cm^{-1}; while the N9-O rocking occurs at 358 cm^{-1}. There is a strong N9-N6 stretching mode at 992 cm^{-1} and a C12-N6 stretch at 1152 cm^{-1}.

The C12-N wagging mode is found at 669 cm^{-1} and the C12-N bending mode is observed at 1318 cm^{-1}. The N8-C15 stretching modes are found at 651 cm^{-1}, 947 cm^{-1} and 1051 cm^{-1}. The Raman band at 310 cm^{-1} shows a bending mode involving N5, C12 and O4. Similar bending and wagging vibrations are also seen at 443 cm^{-1}. The out of plane N-H wagging vibrations (N6H20 and N5H18) are observed at 651 cm^{-1}, 514 cm^{-1} and 577 cm^{-1}. The in-plane N-H bending modes are observed at 1051, 1248, 1318, 1422 and 1532 cm^{-1}.

SERS of Clothianidin

The SERS of clothianidin solutions was investigated using our SERS substrates. Figure 2 (b) shows the SERS spectra for 10 μg/mL of clothianidin. The major peaks are well resolved and the large characteristic peaks compare well to the bulk Raman spectrum. These SERS peaks were matched to the Raman active vibrational modes assigned in Table 1. We expect a shift in wavenumber for the SERS peaks for a solution compared to the bulk Raman spectrum. This is due to the adsorption of clothianidin to the SERS substrate Ag surface via nitrogen atoms in the nitroguanidine structure. The largest shifts in the vibrational modes of the SERS spectra were for those modes involving the atoms in the nitroguanidine moiety. This is typical when employing surface enhanced Raman techniques.

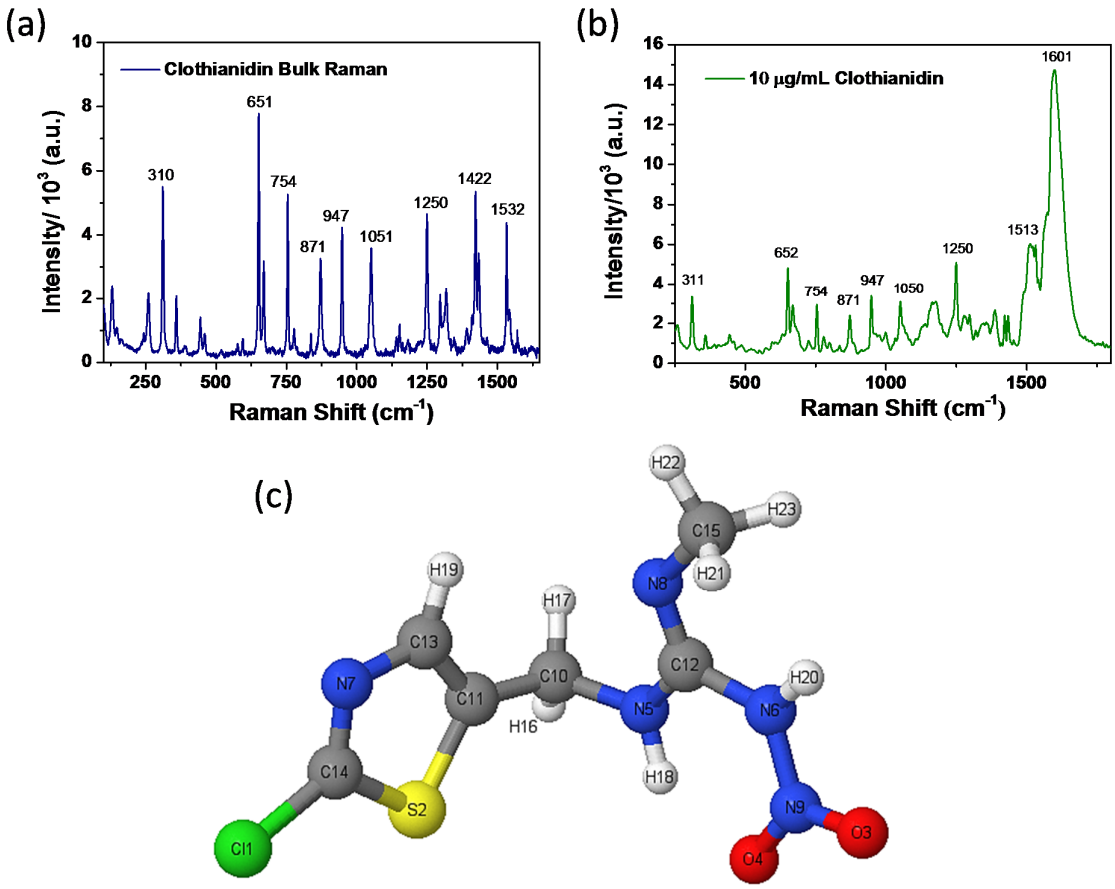

Figure 2: (a) Bulk Raman spectrum and (b) SERS spectrum (10 µg/mL) of clothianidin using fabricated silver coated PVDF substrates. (c) Atomic structure of Clothianidin with atomic numbering.

Raman / cm^{-1}	SERS (1ng) / cm^{-1}	DFT (scaled) / cm^{-1}	Mode Assignments
1570	1605.44	1669/1604	νN9O3O4 as; δN6H20; δN5H18
1532.18	1557.42	1517.25	νC11C13; νC10C11; δC13H19 (ip); δN5H18; νN7C14;
1433.75		1413.35	νN7C14; νC11C13; τC10H17,18
1422.27	1423.91	1403	δC15H21-23; δN6H20
1318.07	1335.62	1317	νN6N9; νN9O3,4 sym; δN8C12N5N6 ; δC5H18 (ip); ωC10H16 (oop)
1296	1304.89	1297	δC10C11C13; τC10H16,17 (oop); δC13H19
1248.83	1254.79	1237	τ C10H16,17 (oop); δC13H19 (ip); δN6H18; δC6H20
1152.94	1176.3	1148/1126	νC10C11; ρC10H16,17 (ip); δC13C11C10; νC11S2; νN6C12; δC13H19 (ip); νC13N7
1051.39	1047.63	1051.46	νHC15N8; νC10N5; δN5H18 (ip); τC10H16,17 (oop);
992	997.961	997.65	νN15N19; νN9O3O4 sym; ωC15H21-24; νC14S2Cl1 as; δN7C14C13H19
947.319	946.846	931.8	ρC10H16,17 (ip); δN5H18 (ip); νC15N8; δC10C11C13
871.121		867.64	ωC13H19 (oop)
754.219	758.308	750.01	ωN6N9O3O4
669		678	ωC12N5N6N8; ωC12N5C10C11; ρC10H16,17; νS2C11C14 as; ωC13H19
651.745	650.094	671.83	δN5C12C10H; ωN5H18 (oop); νS2C11C14 sym; νHN6N9O3; νN8C15
594	573.195	589	ωC10C11C13; ωHC13N7C14; ωC11C13N7C14; ωC13N7C14Cl1
577	556.784	545.78	ωN6H20; ωN5H18; ωS2C11C14; νC14Cl1
514	522.681	514	ωN6H20; ωN5H18
443	432.592	453	ωC11C13N7C14; ωH19C13N7C14S2; νC14Cl1; ωC12N5H18C10; δN6N9O3;
358.837	358.797	339.41	ρN9O3O4; ωC13N7C14Cl1; ωC14Cl1; ωHC10; δC12N6N9; ωC10C11S2; ωC12N5C10C11
310.554	310.513	292.69	δC12N6N9O4; δN6C12N8C15H; ωC12N5H18C10; δS2C14Cl1
259.539	238.755	237.97	ρC10H16,17; δS2C14Cl1; δN8C15H

Table 1: Raman assignations for Clothianidin. The abbreviations are ν, stretching; ω, wagging; τ, twisting; ρ, rocking; δ, bending/scissoring; ip, in plane and oop, out of plane modes. sym and asym denote symmetric and asymmetric modes, respectively.

3.3. Raman and SERS Analysis of Imidacloprid

Figure 3 shows the bulk Raman spectrum for Imidacloprid and the SERS detection of a 10 µg/mL solution in (a) and (b) respectively. The imidacloprid molecule consists of a chloropyridine ring linked with a carbon to an imidazole ring structure. For the purpose of assigning the Raman modes, we name these structures, ring 1 and ring 2, respectively. The structure of imidacloprid, with the atomic numbering used is shown in Figure 4 (c).

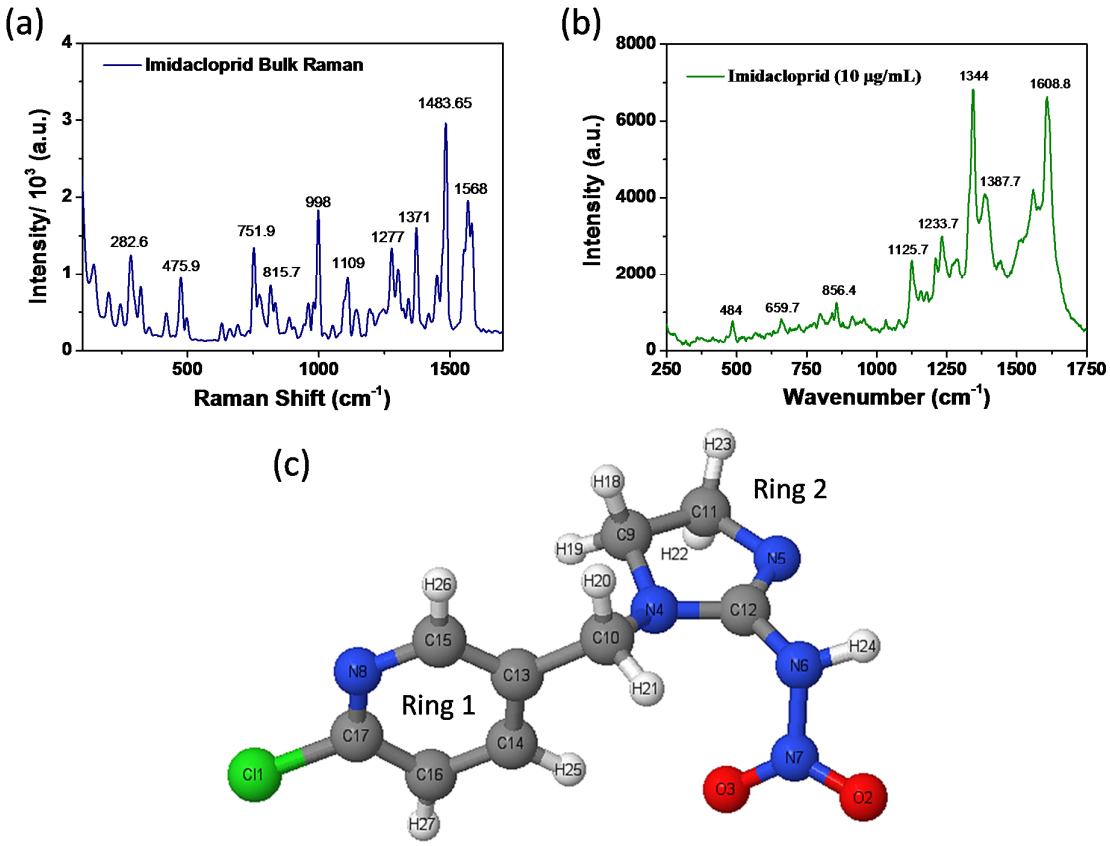

Figure 3: (a) Bulk Raman spectrum and (b) SERS spectrum (10 µg/mL) of imidacloprid using fabricated silver coated PVDF substrates. (c) Structure of imidacloprid with atomic numbering.

The assignments of the key Raman modes are summarised below, and in detail in the SI (Section S3). The Raman spectrum was compared with the SERS spectrum and the DFT results and the assignments are presented in Table 2. [48-50]. Similar to clothianidin, the adsorption of imidacloprid to the SERS substrate will be expected to shift some Raman modes. Typically for molecules that contain a pyridine

ring, attachment to the metal surface is via N in pyridine [51]. We expect that the largest shifts the SERS spectra will be observed with Raman vibrational frequencies relating to Ring 1. This is again due to the adsorption of imidacloprid to the SERS substrate Ag surface via nitrogen atoms in the nitroguanidine structure.

Raman / cm^{-1}	SERS / cm^{-1}	DFT (Scaled) / cm^{-1}	Vibrational Assignments
1584.45	1607	1632/ 1606	νC12N4N5N6 as; δN6H24; νN7O2O3 as
1568.09	1568	1575/1547	CCC Stretching: νC13C14C15 as; νC17N8C16 as
1483.65	1464.07	1483.311621	δC9H19,H18; δC11H23,H22
1451		1448.909319	νC16C17C14 as; νC17N8; δHC14; δHC15; δHC16; δC10H20,H21
1371	1409	1376	νC16C17C14 sym; νC15N8C13 sym; ωC10H20H21
1302	1356.27	1320/1282	ωC9H19H18; ωC11H22H23; ωC10H20H21; δC14H25; νN7O2O3 sym
1277	1327	1279.75	νN7O2O3 sym; ωC9H1918; τC11H22H23; τC10H20H21; δHC15; δHC16
1241	1298.03	1253.77	Ring 1 stretching; τC10H20H21; ωC9H1918; ωC11H22H23; νC12N4N5N6 as; νN6N7
1195	1218	1217.61	τC9H18H19; τC11H22H23
1142	1190.94	1197	νC10C13; νC10C13C14C15 as; ωC10H20; ωC14H25; ωC15H26; ωC16H27;
1109	1162	1125.97	δH25C14C16H27; νC14C16;
998.43	987	1008.09	δC17C16N8; δC13C14C15
815	799	815.11	δC17C16N8, νC13C14C15C10 sym; νC17Cl1; ρC9H18H19; ρC11H23H24
751.931	740.628	768.22	O3O2N7N6 oop; Ring 2 breathing: [δN6N7C12, δC11N5C9]; ρC11H22H23; ρC9H18H19; δC10N4C13
691	677	683	C12N4N5N6 oop; ρC9C11-H sym; δC10N4; Ring 1 breathing: [δC10C14C15, νC17Cl1]
660	661	662/654	ωC12N4N5N6 oop; δC9C11N4; νC13C14C15; νC17Cl1; δC10N4C13
631	635	622	δN8C17C15; δC14C13C16; δC12N4C9C11
475.898	502.089	453	Ring 2 rocking: [ρC10N4C12N6 ρN6C12N4N5] δC13C10N4C12; νC17Cl1; ωC13C14C15; τN8C17C15;
320	320	306	ωN4C12N5; δN4C10C9 oop, δC12N5N16]; δC12N6N7O3

282.658	282.813	274	ρC10H20H21; ρC11H22H23; δC17Cl1
142.932	133.193	144.91	δN6N7O3; ρC11H22H23; ρC10C13N4

Table 2: Raman and SERS assignations for imidacloprid. The abbreviations are ν, stretching; ω, wagging; τ, twisting; ρ, rocking; δ, bending/scissoring; ip, in plane and oop, out of plane modes sym and asym denote symmetric and asymmetric modes, respectively.

C-H vibrations

The stretching modes for C14, C15 and C16 C-H bonds are visible in the extended spectral range at frequencies above ~3000 cm^{-1} , see Figure S4 in the SI, which is typical for C-H hetero-aromatic stretching vibrations.[52]. The in-plane bending vibrations are observed at 1451 cm^{-1}, 1371 cm^{-1} and 1277 cm^{-1}while out of plane wagging modes for the pyridine ring (ring 1) are observed at 1142 cm^{-1}.

Raman modes at 2951 cm^{-1} and 2970 cm^{-1} correspond to C-H symmetric and asymmetric stretching modes involving C9H and C11H. The strong in plane bending vibration for C9-H and C11-H appears as at 1484 cm^{-1}. A twisting vibrational mode was also observed at 1195 cm^{-1}. Finally multiple C9-H and C11-H in-plane rocking modes were observed at 815 cm^{-1}, 751 cm^{-1}, 691 cm^{-1} and 142 cm^{-1}.

The C10 symmetric stretching modes with H21 and H20 were observed at 3008 cm^{-1} and 2878 cm^{-1}, respectively. The only C10H bending vibration is found at 1451 cm^{-1}.

Ring Vibrations

Raman modes at 1568 cm^{-1}, 1451 cm^{-1} and 1371 cm^{-1} are attributed to two asymmetric and one symmetric stretching modes in ring 1. Other stretching modes in Ring 1 are observed at 1142 cm^{-1} and 815 cm^{-1}.

The peaks at 998 cm^{-1} and 691 cm^{-1} are attributed to weak ring bending vibrations in Ring 1. Finally, the Raman peak at 631 cm^{-1} arises from a strong symmetric bending mode of C14 with C13/ C16 and N8 with C15/ C17. The Raman band at 476 cm^{-1} is attributed to wagging of C13 and C17 atoms out of plane in ring 1.

Due to the orientation of imidacloprid, the majority of the imidazole ring vibrational modes (ring 2) are observed as out-of plane vibrations. In-plane rocking and breathing modes are observed at 475 cm^{-1} and 751 cm^{-1}, respectively. The 320 cm^{-1} band is assigned as a ring wagging. A strong C12-N asymmetric stretch is observed at 1584 cm^{-1} and a weaker asymmetric stretch is at 1241 cm^{-1}. The common C12-N wagging vibrations are at 691 cm^{-1} and 660 cm^{-1}.

N-O and C-N Vibrations

The N7-O symmetric and asymmetric stretching vibrations occur at 1302 cm^{-1}[11] and 1584 cm^{-1}, respectively. These are two well resolved bands in both the Raman and SERS spectra, and compare well to the nitroalkane stretching mode reported in the literature.[52] The out of plane wagging vibration of N7-O is observed at 751 cm^{-1}; while the bending vibration of N6-N7-O2-O3 occurs at 142 cm^{-1}. The N6-N7 stretching mode is observed at 1241 cm^{-1}, with a second strong stretching mode at ~1050 cm^{-1}. A strong in-plane N6N7O2 bending mode is seen at 443 cm^{-1}.

3.4. SERS Detection of Neonicotinoids

Having demonstrated that SERS is able to discriminate the presence of our target neonicotinoids at high concentrations, we explore the use of SERS for the quantitative detection of clothianidin and imidacloprid in solution at low concentrations that are relevant for the allowed concentrations of neonicitinoids, up to 1 ng/mL. The SERS spectrum of clothianidin is shown in Figure 4 (a).

Although the Raman peaks are not particularly well resolved or strong at below 940 cm-1, there are clear strong peaks at 946, 1176, 1335, 1557 and 1605 cm-1, which correspond to the previously established characteristic peaks of clothianidin at 947, 1152, 1318, 1532 and 1570 cm-1 in the Raman spectrum. These peaks therefore act as a fingerprint for the presence of clothianidin in solution. This finding demonstrates that clothianidin can be detected by our SERS sensors at these previously unreachable concentrations using a simple drop and dry method.

In a similar manner, the SERS spectrum for a solution of 1 ng/mL of imidacloprid is presented Figure 4 (b). Again the peaks at high wavenumbers, beyond 1200 cm-1 which correspond to the characteristic peaks of the molecule, are well resolved. Bands at 1218, 1355, 1408, 1464, 1571 and 1605 cm-1, labelled in Figure 4 (b), are similar to those in the bulk Raman spectrum (refer back to Figure 2 (a)). They are mainly attributed to the bending and wagging of the ring structures in imidacloprid.

A key result is that this limit of detection is significantly lower than the current lowest legal residue limit of *ca.* 10 ng/mL for food products [53] which demonstrates the power of SERS technique for the detection of neonicotinoid residues, even if the legal limit were to be lowered towards 1mg/mL.

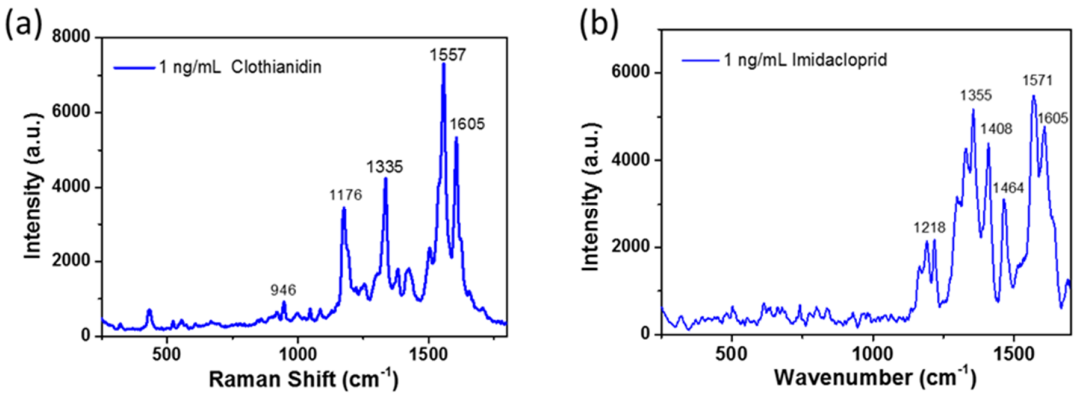

Figure 4: SERS detection of (a) clothianidin and (b) imidacloprid at 1 ng/mL using the fabricated silver coated PVDF substrates.

3.5. Comparison with other Techniques

The results for neonicotinoid detection obtained using our nanowire array SERS devices are compared against literature reports and Table 3 presents typical limits of detection. The measured limit of detection for the present SERS devices is a significant improvement over solid state electrochemical measurements and on a par with results achieved using high-end laboratory instrumentation, but with the advantage of low cost and potential in situ use of the sensor devices. The use of SERS to detect the presence of these neonicotinoids gives a very useful, accurate, and potentially *in-situ*, analytical tool and clearly demonstrates the viability of this approach to the selective detection of neonicotinoid species.

Detection method	Electrode Type/ Diameter	Neonicotinoid	LOD	Ref
Enzyme-linked immunosorbent assays	-	Imidacloprid	20 nM	20
	-	Clothianidin	11 nM	54
Gas Chromatography – Mass Spectroscopy	-	Clothianidin	40 nM	28
Tandem Mass Spectrometry	-	Clothianidin	40 nM	55
High performance liquid chromatography	-	Imidacloprid	90 nM	56
	-	Imidacloprid	39 nM	57
	-	Clothianidin	10 nM	58
Differential-Pulse Voltammetry	Bismuth-Film Modified GCE	Clothianidin	3000 nM	59
	Carbon paste electrode (d = 2 mm)	Imidacloprid	2030 nM	56

	Hanging Mercury drop electrode	Imidacloprid	2560 nM	60
	Nanosilver/SDS GCE (d = 3 mm)	Imidacloprid	250 nM	61
	Hanging Mercury drop electrode	Imidacloprid	39 nM	62
Cyclic voltammetry	Glassy carbon Electrode (GCE)	Imidacloprid	10.9 µM	27
	Nanosilver/SDS GCE (d = 3 mm)	Imidacloprid	630 nM	61
	Reduced graphene oxide GCE (d = 3 mm)	Imidacloprid	400 nM	63
Square wave Voltammetry	Silver-Amalgam Film Electrode	Clothianidin	2080 nM	64
	Hanging Mercury drop electrode	Imidacloprid	16 nM	26
Surface Enhanced Raman Spectroscopy (SERS)		Imidacloprid	19.5 nM	65
		Imidacloprid	40 nM	66
		Clothianidin	Not reported previously	
		Imidacloprid	**4 nM**	**This**
		Clothianidin	**4 nM**	**work**

Table 3: Comparison of detection methods for clothianidin and imidacloprid in the literature compared with our results.

4. Conclusion

The use of Surface Enhanced Raman Spectroscopy in the development of low cost, portable sensor devices that can be used in the field for nitroguanidine neonicotinoid insecticide detectionis appealing. To make progress towards this goal, this paper presents an analysis of the bulk Raman and SERS spectra of two neonicotinoids, namely clothianidin and imidacloprid, together with the use of SERS to demonstrate the sensing of these molecules at concentrations as low as 1 ng / L.

Silver nanostructured surfaces were fabricated for qualitative SERS, which provides the characteristic spectra of the target molecules. Combined with first principles simulations, this allowed assignment of all Raman spectral modes for both molecules. To our knowledge, this is the first report of SERS analysis and vibrational assignment of Clothianidin and we demonstrate the feasibility of SERS sensing down to concentrations of 1 nM.

The limits of detection were validated through SERS analysis on the prepared aqueous solutions, with limits of detection of 1ng/mL for both compounds. These detection limits are significantly lower than reported solid state electrochemical techniques and are on par with high-end chromatographic-mass spectroscopy laboratory methods. These SERS sensors thus allow for the selective and sensitive detection of neonicotinoids, and provides complimentary qualitative and quantitative data for the molecules. Furthermore, this technique can be adapted to portable devices for remote sensing applications. Further work focuses on integrating our device with an electronics platform for truly portable residue detection.

Supporting Information

The Supporting Information is available free of charge at https://pubs.acs.org/doi/10.1021/acs.xxxxx.

SERS sensor Characterisation with Crystal Violet, full Clothianidin vibrational analysis, full imidacloprid vibrational analysis (PDF).

5. Acknowledgments

This publication has emanated from research supported in part by a research grant from Science Foundation Ireland (SFI) under Connect (13/RC/2077), the VistaMilk Centre Science Foundation Ireland (SFI); Department of Agriculture Food and the Marine (DAFM) under Grant Number 16/RC//3835, the Technology Innovation Development Award (SFI/12/TIDA12377) and Environmental Protection Agency UisceSense (EPA 2015-W-MS-21)

6. References

1. A. Elbert, M. Haas, B. Springer, W. Thielert and R. Nauen, *Pest Management Science*, 2008, **64**, 1099-1105.
2. P. Jeschke and R. Nauen, *Pest Management Science*, 2008, **64**, 1084-1098.
3. R. Nauen and T. Bretschneider, *Pesticide Outlook*, 2002, **13**, 241-245.
4. M. Tomizawa and J. E. Casida, *Annu. Rev. Pharmacol. Toxicol.*, 2005, **45**, 247-268.
5. M. Henry, M. Beguin, F. Requier, O. Rollin, J.-F. Odoux, P. Aupinel, J. Aptel, S. Tchamitchian and A. Decourtye, *Science*, 2012, **336**, 348-350.
6. P. R. Whitehorn, S. O'Connor, F. L. Wackers and D. Goulson, *Science*, 2012, **336**, 351-352.
7. L. Miligi, A. S. Costantini, A. Veraldi, A. Benvenuti, Will and P. Vineis, *Annals of the New York Academy of Sciences*, 2006, **1076**, 366-377.
8. R. Meinert, J. Schüz, U. Kaletsch, P. Kaatsch and J. Michaelis, *American Journal of Epidemiology*, 2000, **151**, 639-646.
9. R. Betarbet, T. B. Sherer, G. MacKenzie, M. Garcia-Osuna, A. V. Panov and J. T. Greenamyre, *Nat Neuro*, 2000, **3**, 1301-1306.
10. P. Salameh, I. Baldi, P. Brochard, C. Raherison, B. A. Saleh and R. Salamon, *European Respiratory Journal*, 2003, **22**, 507-512.
11. J. Kimura-Kuroda, Y. Komuta, Y. Kuroda, M. Hayashi and H. Kawano, *Plos One*, 2012, **7**, e32432.
12. V. Duzguner and S. Erdogan, *Pesticide Biochemistry and Physiology*, 2010, **97**, 13-18.
13. W. Hanke and J. Jurewicz, *International Journal of Occupational Medicine and Environmental Health*, 2004, **17**, 223-243.
14. T. Blacquiere, G. Smagghe, C. A. van Gestel and V. Mommaerts, *Ecotoxicology*, 2012, **21**, 973-992.
15. T. J. Wood and D. Goulson, *Environmental Science and Pollution Research*, 2017, **24**, 17285-17325.
16. European Commission, *Official Journal of the European Union*, 2013, **139**, 12-14.
17. I. Ferrer, E. M. Thurman and A. R. Fernández-Alba, *Analytical Chemistry*, 2005, **77**, 2818-2825.

18. European Food Safety Authority, *EFSA Journal*, 2016, **14**, e04611-n/a.
19. European Food Safety Authority, *EFSA Journal*, 2018, **16**, e05177.
20. J. K. Lee, K. C. Ahn, O. S. Park, S. Y. Kang and B. D. Hammock, *J Agr Food Chem*, 2001, **49**, 2159-2167.
21. E. Watanabe, K. Baba, H. Eun and S. Miyake, *Food Chemistry*, 2007, **102**, 745-750.
22. H. Obana, M. Okihashi, K. Akutsu, Y. Kitagawa and S. Hori, *J Agr Food Chem*, 2002, **50**, 4464-4467.
23. S. Liu, Z. Zheng, F. Wei, Y. Ren, W. Gui, H. Wu and G. Zhu, *J Agr Food Chem*, 2010, **58**, 3271-3278.
24. A. Aguera, E. Almansa, S. Malato, M. Maldonado and A. Fernandez-Alba, *Analysis*, 1998, **26**, 245-251.
25. A. Navalón, A. González-Casado, R. El-Khattabi, J. L. Vilchez and A. R. Fernández-Alba, *The Analyst*, 1997, **122**, 579-581.
26. A. Guiberteau, T. Galeano, N. Mora, P. Parrilla and F. Salinas, *Talanta*, 2001, **53**, 943-949.
27. V. J. Guzsvány, F. F. Gaál, L. J. Bjelica and S. N. Ökrész, *Journal of the Serbian Chemical Society*, 2005, **70**, 735-743.
28. L. Li, G. Jiang, C. Liu, H. Liang, D. Sun and W. Li, *Food Control*, 2012, **25**, 265-269.
29. Z. Papp, V. Guzsvány, I. Svancara and K. Vytras, *Journal of Agricultural Science and Technology*, 2011, **5**, 85-92.
30. J. L. Ví lchez, M. C. Valencia, A. Navalón, B. Molinero‐Morales and L. F. Capitán-Vallvey, *Anal Chim Acta*, 2001, **439**, 299-305.
31. M. G. Albrecht and J. A. Creighton, *J Am Chem Soc*, 1977, **99**, 5215-5217.
32. M. Fleischmann, P. J. Hendra and A. J. McQuillan, *Chem Phys Lett*, 1974, **26**, 163-166.
33. A. Otto, I. Mrozek, H. Grabhorn and W. Akemann, *Journal of Physics: Condensed Matter*, 1992, **4**, 1143.
34. P. L. Stiles, J. A. Dieringer, N. C. Shah and R. P. V. Duyne, *Annu. Rev. Anal. Chem.*, 2008, **1**, 601-626.
35. N. C. Creedon, P. Lovera, A. Furey and A. O'Riordan, *Sensors and Actuators B: Chemical*, 2018, **259**, 64-74.
36. A. D. Becke, *The Journal of chemical physics*, 1993, **98**, 5648-5652.
37. F. Weigend and R. Ahlrichs, *Physical Chemistry Chemical Physics*, 2005, **7**, 3297-3305.
38. J. F. Pepin, A. Riou and T. Renault, *Journal of virological methods*, 2008, **149**, 269-276.
39. S. Grimme, *Journal of computational chemistry*, 2006, **27**, 1787-1799.
40. C. Peng, P. Y. Ayala, H. B. Schlegel and M. J. Frisch, *Journal of Computational Chemistry*, 1996, **17**, 49-56.
41. P. Deglmann, F. Furche and R. Ahlrichs, *Chemical physics letters*, 2002, **362**, 511-518.
42. P. Deglmann and F. Furche, *The Journal of Chemical Physics*, 2002, **117**, 9535-9538.
43. J. P. Merrick, D. Moran and L. Radom, *The Journal of Physical Chemistry A*, 2007, **111**, 11683-11700.
44. L. S. Khaikin, O. E. Grikina, B. V. Lokshin, K. P. Dyugaev and A. M. Astakhov, *Russian Chemical Bulletin*, 2008, **57**, 499-505.
45. F. Zhang, Y. Zhang, H. Ni, K. Ma and R. Li, *Spectrochimica Acta Part A: Molecular and Biomolecular Spectroscopy*, 2014, **118**, 162-171.
46. G. Socrates, *Infrared and Raman Characteristic Group Frequencies: Tables and Charts*, John Wiley & Sons, 2001.
47. X.-M. Zhu, S.-Q. Zhang, X. Zheng and D. L. Phillips, *The Journal of Physical Chemistry A*, 2005, **109**, 3086-3093.
48. L. M. Markham, L. C. Mayne, B. S. Hudson and M. Z. Zgierski, *The Journal of Physical Chemistry*, 1993, **97**, 10319-10325.
49. N. Sundaraganesan, S. Ilakiamani, B. Anand, H. Saleem and B. D. Joshua, *Spectrochimica Acta Part A: Molecular and Biomolecular Spectroscopy*, 2006, **64**, 586-594.

50. M. Kumar, M. Srivastava and R. A. Yadav, *Spectrochimica Acta Part A: Molecular and Biomolecular Spectroscopy*, 2013, **111**, 242-251.
51. L. Chen, Y. Gao, H. Xu, Z. Wang, Z. Li and R.-Q. Zhang, *Physical Chemistry Chemical Physics*, 2014, **16**, 20665-20671.
52. D. Lin-Vien, N. B. Colthup, W. G. Fateley and J. G. Grasselli, *The handbook of infrared and Raman characteristic frequencies of organic molecules*, Elsevier, 1991.
53. European Food Safety Authority, *EFSA Journal 2014*, 2014, **12**, 3694.
54. M. Li, E. Sheng, L. Cong and M. Wang, *J Agr Food Chem*, 2013, **61**, 3619-3623.
55. B. M. Kim, J.-S. Park, J.-H. Choi, A. M. Abd El-Aty, T. W. Na and J.-H. Shim, *Food Chemistry*, 2012, **131**, 1546-1551.
56. Z. Papp, I. Švancara, V. Guzsvány, K. Vytřas and F. Gaál, *Microchim Acta*, 2009, **166**, 169-175.
57. H. Obana, M. Okihashi, K. Akutsu, Y. Kitagawa and S. Hori, *J Agr Food Chem*, 2003, **51**, 2501-2505.
58. M.-F. Chen, J.-W. Huang, S.-S. Wong and G.-C. Li, *Journal of Food and Drug Analysis*, 2005, **13**, 279-283.
59. V. Guzsvány, Z. Papp, J. Zbiljić, O. Vajdle and M. Rodić, *Molecules*, 2011, **16**, 4451.
60. L. Kashid and N. Pawar, *International Journal of Scientific and Research Publications*, 2015.
61. A. Kumaravel and M. Chandrasekaran, *Sensors and Actuators B: Chemical*, 2011, **158**, 319-326.
62. A. Navalón, R. El-Khattabi, A. González-Casado and J. Vilchez, *Microchim Acta*, 1999, **130**, 261-265.
63. L. Kong, X. Jiang, Y. Zeng, T. Zhou and G. Shi, *Sensors and Actuators B: Chemical*, 2013, **185**, 424-431.
64. M. Brycht, O. Vajdle, J. Zbiljić, Z. Papp, V. Guzsvány and S. Skrzypek, *International Journal of Electrochemical Science*, 2012, **7**.
65. R. Hou, S. Pang and L. He, *Anal Methods*, 2015, **7**, 6325-6330.
66. H. Zhang, Y. Kang, P. Liu, X. Tao, J. W. Pei, H. Li and Y. P. Du, *Anal Lett*, 2016, **49**, 2268-2278.